Image-Based Vehicle Verification Using Steerable Gaussian Filter

Heri Prasetyo, Wiranto and Winarno
Department of Informatics, Universitas Sebelas Maret (UNS), Surakarta, Indonesia.
heri.prasetyo@staff.uns.ac.id

***Abstract*—This paper presents a new feature descriptor for a vehicle verification system. The Steerable Gaussian Filter (SGF) is utilized to generate an image feature descriptor. The descriptor is constructed by concatenating the statistical parameters of the SGF filtered output. The Maximum Likelihood Estimation (MLE) estimates the statistical estimator using a heavy-tailed and bell-shaped distribution assumption such as Gaussian, Laplace, or Generalized Gaussian Distribution (GGD). A classifier assigns a class label of the vehicle hypothesis based on an image descriptor. As documented in the experimental results, the proposed feature descriptor achieves a promising result, and it outperforms the state-of-the-art vehicle verification systems, making it a very competitive candidate in the practical applications.**

***Index Terms*—Maximum Likelihood Estimation; Steerable Gaussian Filter; Supervised Classification; Vehicle Verification.**

I. INTRODUCTION

Several approaches have been proposed in the literature to handle the vehicle detection and verification issues. A complete survey of the image-based vehicle detection is addressed in [1]. The vehicle detection searches the potential locations of vehicles in a given image. It produces the vehicle hypothesis which needs a further verification process to determine whether it is a correct vehicle or an outlier occurring in the vehicle detection stage. For this purpose, some methods have been proposed in [1-5] to verify the correctness of the vehicle hypothesis in image-based vehicle detection. In the vehicle verification process, the feature descriptor of an image is simply composed of the statistical parameters of the Gabor filtered magnitude for all scales and orientations sub-bands [4-5]. The Gabor-based vehicle verification yields a good verification result as reported in [1-8].

In this paper, the local features are generated from the SGF filtered output for the vehicle verification task. The first and second order derivative of the SGF is utilized to construct an image feature descriptor. In the vehicle verification system, a set of vehicle candidates or vehicle hypotheses of a given input image are firstly detected using some vehicle or object moving detection. These hypotheses are further examined in the vehicle verification module to determine the correctness of the vehicle occurrence. In our proposed method, an image descriptor is constructed by stacking the distribution estimators over all SGF filtered outputs. The feature descriptor of each vehicle hypothesis is subsequently fed into a classifier module which assigns a class label by taking a trained set of feature descriptor into account. The classifier identifies whether the vehicle hypothesis falls into the correct vehicle class or stands as a non-vehicle object.

II. STEERABLE GAUSSIAN FILTER AND ITS STATISTICAL MODELING

This section presents a brief introduction of the Steerable Gaussian Filter (SGF) and its statistical modeling of SGF output over several distribution assumptions such as, Gaussian, Laplace, and Generalized Gaussian Distribution (GGD). The estimator of bell-shape and heavily-tailed distribution is estimated by means of Maximum Likelihood Estimation (MLE) method from the SGF filtered output.

A. Steerable Gaussian Filter

The Gaussian-like filter can be derived from a linear combination of basis filters [9-11]. The two-dimensional circularly symmetric Gaussian function is defined as:

$$G(x,y) = \exp\{-(x^2+y^2)\} \tag{1}$$

where $G(x,y)$ = two dimensional Gaussian function
x, y = spatial coordinat

The first-order derivative of $G(x,y)$ in x is given as:

$$G_1^{0^\circ} = \frac{\partial}{\partial x} G(x,y) = -2x \exp\{-(x^2+y^2)\} \tag{2}$$

where $G_1^{0^\circ}$= first-order derivative of $G(x,y)$ in x

Whereas, the first-order derivative of $G(x,y)$ in y can be computed as:

$$G_1^{90^\circ} = \frac{\partial}{\partial y} G(x,y) = -2y \exp\{-(x^2+y^2)\} \tag{3}$$

where $G_1^{90^\circ}$= first-order derivative of $G(x,y)$ in y

A separable filter G_1^θ is obtained by computing a linear combination of $G_1^{0^\circ}$ and $G_1^{90^\circ}$ at an arbitrary orientation θ as:

$$G_1^\theta = \cos(\theta)\, G_1^{0^\circ} + \sin(\theta)\, G_1^{90^\circ} \tag{4}$$

where θ= a rotated angle from the origin with the bound of $0 \leq \theta \leq \pi$

The function G_1^θ is called as a basis filter which is subsequently be interpolated with $\cos(\theta)$ and $\sin(\theta)$ function to produce a set of filter banks. We refer G_1^θ as the first-order of Steerable Gaussian Filter (SGF-1). To generate a set of SGF responses on image I, a convolution is performed on image I with the basis filter G_1^θ. Since the convolution is a linear operator, the SGF filtered response can be obtained as:

$$R_1^{0^\circ} = I * G_1^{0^\circ} \tag{5}$$

$$R_1^{90^\circ} = I * G_1^{90^\circ} \quad (6)$$

where $*$= convolution process

Subsequently, the SGF response of image I is computed as:

$$R_1^{\theta} = \cos(\theta)\, R_1^{0^\circ} + \sin(\theta)\, R_1^{90^\circ} \quad (7)$$

where R_1^{θ}=two-dimensional SGF-1 response

The second derivative of SGF (SGF-2) has been demonstrated to yield a bandpass filter, and offers a directionality to some extent. The SGF-2 is formally defined as:

$$G_2^{\theta} = \cos^2(\theta)\, G_{xx} - 2\cos(\theta)\sin(\theta)\, G_{xy} + \sin^2(\theta)\, G_{yy} \quad (8)$$

where G_2^{θ}=basis filter of SGF-2
G_{xx}=second-order derivative of $G(x, y)$ at x-x
G_{xy}=second-order derivative of $G(x, y)$ at x-y
G_{yy}= second-order derivative of $G(x, y)$ at y-y

To generate the local feature of image I, the filtering process of I with SGF-2 can be performed as:

$$R_2^{\theta} = I * G_2^{\theta} \quad (9)$$

where R_2^{θ}=the filtering result with the second-order derivative of Gaussian-like filter (SGF-2 response)

Multiple SGF responses can be obtained by adjusting the multiple orientation angles θ. Figure 1 shows an example of the SGF-1 and SGF-2 filtered outputs and its responses with $\theta = \frac{\pi}{4}, \frac{\pi}{2}, \frac{3\pi}{4}, and\ \pi$. In our proposed method, an image feature descriptor is constructed from the statistical estimator of SGF filtered output. The MLE produces the statistical estimator of SGF filtered output for each orientation angle θ.

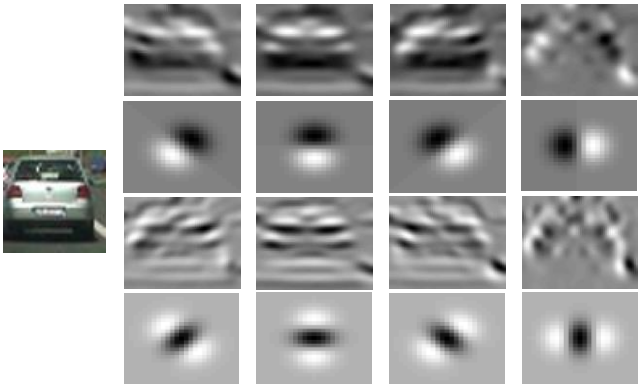

Figure 1: The first and third row are filtered images resulting from SGF-1 (first row) and SGF-2 (third row), respectively, with corresponding its responses (shown at the second and fourth rows). The second to fifth column are the results over different values $\theta = \left\{\frac{\pi}{4}, \frac{\pi}{2}, \frac{3\pi}{4}, \pi\right\}$. The first column represents an input image.

B. MLE with Gaussian and Laplace Distribution

A simple and naïve approach to describe the marginal distribution of SGF filtered output is with the Gaussian or Laplace distribution assumption. The MLE with Gaussian distribution assumption produces two distribution estimator, namely mean value ($\hat{\mu}$) and standard deviation ($\hat{\sigma}$), for each SGF filtered output. Let $X = \{x_1, \dots, x_N\}$ be a set of "independent and identically distributed" (i.i.d.) sample points drawn from SGF filtered output. The value of X can be set with SGF-1 or SGF-2 coefficients. The formal procedure of MLE is maximizing the log-likelihood function of set X by taking the first-order derivative of log-likelihood function and setting it by zero to estimate the distribution estimator. The log-likelihood function of X is derived as:

$$\mathcal{L}(\mu, \sigma|X) = -\frac{1}{2}N\log 2\pi - N\log\sigma - \frac{\sum_{i=1}^{N}(x_i-\mu)^2}{2\sigma^2} \quad (10)$$

where $\mathcal{L}(\mu, \sigma|X)$=log-likelihood function of X with Gaussian assumption

The two estimators of this log-likelihood are given as follow:

$$\hat{\mu} = \frac{\sum_{i=1}^{N} x_i}{N} \quad (11)$$

$$\hat{\sigma} = \sqrt{\frac{\sum_{i=1}^{N}(x_i-\hat{\mu})^2}{N}} \quad (12)$$

where $\hat{\mu}$=the first estimator, i.e. mean value
$\hat{\sigma}$=the second estimator, i.e. standard deviation

An image feature descriptor derived from Gaussian distribution estimator yields promising result in the vehicle verification system as reported in [10]. An alternative choice for describing the SGF filtered output is to use the Laplace distribution which has fatter tail compared to the Gaussian distribution. The Laplace distribution requires the absolute difference terms between the data point and sample mean value to describe its PDF. The log-likelihood function of X under Laplace distributoin assumption is given as:

$$\mathcal{L}(\mu, \lambda|X) = -N\log 2\lambda - \frac{\sum_{i=1}^{N}|x_i-\mu|}{\lambda} \quad (13)$$

where $\mathcal{L}(\mu, \lambda|X)$=log-likelihood function of X with Laplace assumption

The estimators of Laplace distribution can be trivialy obtained as:

$$\hat{\mu} = \text{median}\{x_1, \dots, x_N\} \quad (14)$$

$$\hat{\lambda} = \frac{1}{N}\sum_{i=1}^{N}|x_i - \widehat{\mu}| \quad (15)$$

where $\hat{\mu}$=the first estimator, i.e. median value
$\hat{\lambda}$=the second estimator, i.e. Laplace value
$median\{\cdot\}$= operator to compute median value

In a nutshell, the median value and least-absolute deviation of the sample data can be used to represent the statistical estimator of Laplace distribution. The MLE of Gaussian and Laplace distribution requires simple mathematical operation for computing the distribution estimator.

C. MLE with Generalized Gaussian Distribution

The GGD has been reported to yield promising results in the signal processing and computer vision applications for its ability to adapt two different distributions, i.e., Gaussian and Laplace distribution. The log-likelihood function of X under GGD assumption can be obtained as:

$$\begin{aligned}\mathcal{L}(\alpha,\beta|x) &= \log L(\alpha,\beta|x)\\ &= N\{\log\beta - \log 2\alpha\} + N\left\{\log 1 - \log\Gamma\left(\frac{1}{\beta}\right)\right\}\\ &\quad - \sum_{i=1}^{N}\left(\frac{|x_i|}{\alpha}\right)^{\beta}\end{aligned} \tag{16}$$

where $\mathcal{L}(\alpha,\beta|x)$=log-likelihood function of X under GGD assumption

The MLE under GGD assumption produces two distribution estimators of SGF filtered output as:

$$\hat{\alpha} = \left(\frac{\hat{\beta}}{N}\sum_{i=1}^{N}|x_i|^{\hat{\beta}}\right)^{\frac{1}{\hat{\beta}}} \tag{17}$$

$$1 + \frac{\Psi\left(\frac{1}{\hat{\beta}}\right)}{\beta} - \frac{\sum_{i=1}^{N}|x_i|^{\beta}\log|x_i|}{\sum_{i=1}^{N}|x_i|^{\beta}} + \frac{\log\left(\frac{\beta}{N}\sum_{i=1}^{N}|x_i|^{\beta}\right)}{\beta} = 0 \tag{18}$$

where $\hat{\alpha}$=the first estimator of GGD
$\hat{\beta}$=the second estimator of GGD
$\Psi(\cdot)$= digamma function

The Newton-Raphson method can be utilized to find $\hat{\beta}$ since there is no closed-form for solving Equation (18).

The goodness-of-fit statistical value χ^2 and Kullback-Leibler Divergence (KLD) are employed to measure the fitting accuracy of SGF filtered output. A better statistical fitting result is indicated with a smaller χ^2 or KLD value. Figure 2 shows an example of statistical fitting with Gaussian, Laplace, and GGD assumptions on SGF-1 and SGF-2. As it can be seen in this figure, the GGD yields the best statistical fitting compared to that of Gaussian and Laplace distribution fitting for SGF-1 and SGF-2.

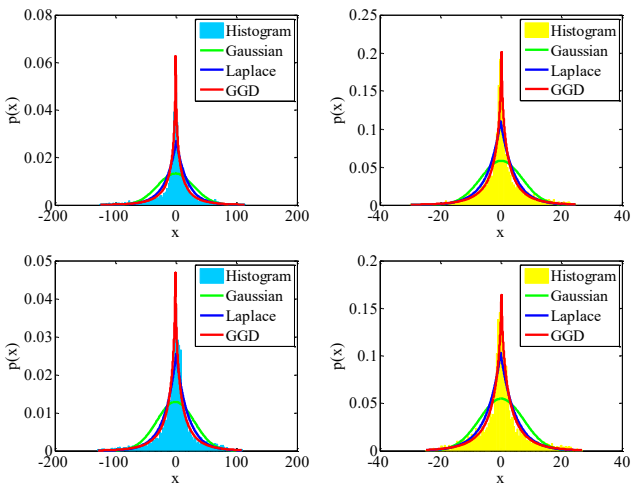

Figure 2: Statistical fitting of SGF-1 (first column) and SGF-2 (second column) under different probability modeling.

III. Proposed Vehicle Verification

In the proposed vehicle verification system, an image feature descriptor is constructed by concatenating the distribution estimator over all SGF filtered outputs. An input image is firstly converted from color to grayscale. The converted image is subsequently fed into the SGF decomposition procedure to acquire SGF filtered outputs along various filter orientations. The MLE estimates the statistical estimator of each SGF output under a specific distribution assumption. An image feature composed from the statistical estimator of SGF filtered output is obtained at the end of feature extraction stage.

Let I be a grayscale input image. The SGF firstly decomposes I into several SGF filtered outputs by performing the convolution between I with the basis filter G_f^{θ} as denoted by:

$$R_f^{\theta} = I * G_f^{\theta} \tag{19}$$

where $f \in \{1,2\}$=the selected order derivative of SGF.

The values $f = 1$ and $f = 2$ indicate SGF-1 and SGF-2, respectively, for the SGF decomposition. The symbol $\theta = \{0,\dots,\pi\}$ denotes the orientation angle, in which the difference between two consecutive angles is denoted as $\Delta\theta$ in the SGF convolution. R_f^{θ} represents the SGF filtered output on orientation angle θ. At the end of SGF decomposition, a set of SGF filtered output R_f^{θ} is obtained over all θ values.

An image feature descriptor is derived from the SGF output R_f^{θ} by means of the MLE under a specific distribution assumption. The MLE procedure is performed for each R_f^{θ} to compute the statistical estimator $\hat{\theta}$. In this paper, three various distributions are investigated for deriving an image feature descriptor, i.e., Gaussian, Laplace, and GGD. The MLE for R_f^{θ} under Gaussian distribution assumption is defined as:

$$\mathcal{M}_{\mu\sigma}\{R_f^{\theta}\} \Rightarrow \{\hat{\mu}_{\theta},\hat{\sigma}_{\theta}\} \tag{20}$$

where $\mathcal{M}_{\mu\sigma}\{\cdot\}$=the MLE computation under Gaussian distribution assumption.

The symbol $\hat{\mu}_{\theta}$ and $\hat{\sigma}_{\theta}$ are the estimated mean value and standard deviation of SGF filtered output upon the orientation angle θ, respectively. As a result, a Gaussian feature descriptor can be constructed by concatenating $\{\hat{\mu}_{\theta},\hat{\sigma}_{\theta}\}$ over all R_f^{θ} sub-bands as follow:

$$F_{\mu\sigma} = \{\hat{\mu}_0,\hat{\sigma}_0,\dots,\hat{\mu}_{\theta},\hat{\sigma}_{\theta},\dots,\hat{\mu}_{\pi},\hat{\sigma}_{\pi}\} \tag{21}$$

where $F_{\mu\sigma}$=Gaussian feature descriptor

The second feature descriptor, namely Laplace feature descriptor, can also be generated using the similar strategy as conducted in the Gaussian descriptor. Herein, the MLE estimates the statistical estimator of SGF filtered output under the Laplace distribution assumption. The MLE of R_f^{θ} under the Laplace distribution assumption is given as:

$$\mathcal{M}_{\mu\lambda}\{R_f^{\theta}\} \Rightarrow \{\hat{\mu}_{\theta},\hat{\lambda}_{\theta}\} \tag{22}$$

where $\mathcal{M}_{\mu\lambda}\{\cdot\}$=the MLE computation under Laplace distribution assumption.

The Laplace feature descriptor can be subsequently derived by concatenating the estimator $\{\hat{\mu}_{\theta},\hat{\lambda}_{\theta}\}$ over all SGF filtered outputs as:

$$F_{\mu\lambda} = \{\hat{\mu}_0,\hat{\lambda}_0,\dots,\hat{\mu}_{\theta},\hat{\lambda}_{\theta},\dots,\hat{\mu}_{\pi},\hat{\lambda}_{\pi}\} \tag{23}$$

where $F_{\mu\lambda}$=Laplace feature descriptor.

The third feature descriptor, namely GGD feature descriptor, can be similarly derived by performing the MLE procedure under GGD assumption over all SGF filtered outputs. In this case, the MLE calculates the GGD estimator using:

$$\mathcal{M}_{\alpha\beta}\{R_f^{\theta}\} \Rightarrow \{\hat{\alpha}_{\theta}, \hat{\beta}_{\theta}\} \tag{24}$$

where $\mathcal{M}_{\alpha\beta}\{\cdot\}$= the MLE computation under GGD assumption.

Subsequently, the GGD feature descriptor can be composed by stacking the GGD estimator $\{\hat{\alpha}_{\theta}, \hat{\beta}_{\theta}\}$ over all SGF filtered outputs as:

$$F_{\alpha\beta} = \{\hat{\alpha}_0, \hat{\beta}_0, \dots, \hat{\alpha}_{\theta}, \hat{\beta}_{\theta}, \dots, \hat{\alpha}_{\pi}, \hat{\beta}_{\pi}\} \tag{25}$$

where $F_{\alpha\beta}$=GGD feature descriptor.

The dimensionalities of the Gaussian, Laplace, and GGD feature descriptors are identical, since the MLE produces the same statistical estimator for each SGF filtered output, i.e., two estimators for each SGF output.

Two major steps are involved in the entire vehicle verification system: 1) vehicle detection, and 2) vehicle verification. The vehicle detection estimates and detects the occurrence of moving object such as vehicle motion, human activity on the road, shadow, tree-leaf motion, fake foreground, etc. using some object tracking or moving detection algorithms. The vehicle detection produces several vehicle hypotheses (vehicle candidates) from a given input image. At the vehicle verification stage, this vehicle hypothesis is further verified and concluded whether they are correct vehicle objects or fake moving objects. Figure 4 shows the general framework of vehicle detection and verification system. Some outliers may occur at the vehicle detection stage. At the vehicle verification, these outliers (fake moving objects) are verified out to acquire the correct decision of the vehicles.

The vehicle verification examines the vehicle hypothesis (vehicle candidates) produced from a vehicle detection using a specific feature descriptor. Figure 3 illustrates the schematic diagram of the proposed vehicle verification system. In this scheme, an image feature descriptor is derived from the statistical estimator of SGF filtered output through the feature extraction stage. This feature descriptor is only computed on a region of vehicle hypotheses (vehicle candidates). A classifier assigns a class label for vehicle hypothesis based on its feature descriptor and the trained feature set. In our system, the vehicle verification can be regarded as a two-class supervised problem. The classifiers assign a "vehicle" or "non-vehicle" label over all vehicle hypotheses. The proposed Gaussian, Laplace, or GGD feature descriptors are utilized for the vehicle verification.

IV. Experimental Results

The effectiveness of the proposed feature descriptor is examined with the open access GTI vehicle image database [12]. This vehicle image database consists of 8000 color images of size 64×64. The database is further divided into two classes, i.e., positive and negative classes. The positive class contains 4000 rear vehicle images with four various poses, i.e., far, left, middle close, and right vehicle poses. The negative class has 4000 non-vehicle images, consisting of the other elements in traffic sequence captured with four different camera views (i.e. far, left, middle close, and right camera view).

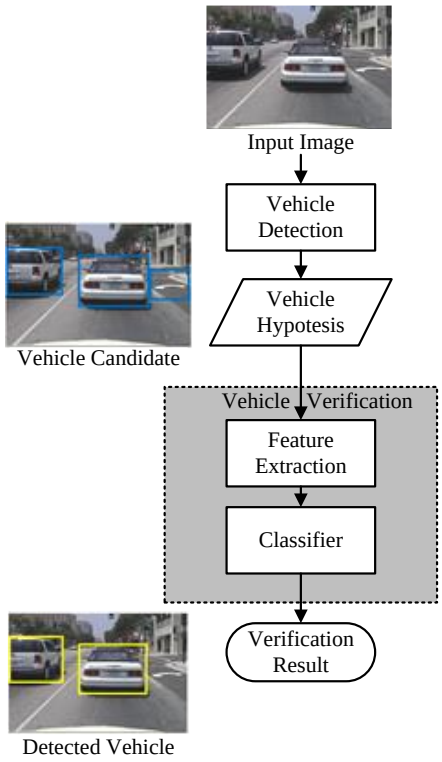

Figure 3: The proposed vehicle verification system

In our experiment, the identical experimental setup is applied, which has been conducted in [2-5]. The verification performance is examined using the 5-fold 50% holdout cross-validation method [4]. The data are split into five folds. Two independent runs are conducted on each fold. For the first run, half of the data is turned as training set, while the other half is considered as testing set. Subsequently, the training and testing sets are interchanged in the second run. The accuracy of the verification system is measured in terms of percentage of correct prediction over all testing images. The final verification accuracy is obtained by averaging the proportion of correct prediction over all folds.

A. *Effectiveness of the Proposed Feature Descriptor*

The effectiveness of proposed feature descriptor for vehicle verification is investigated in this subsection. In our experiment, a color image is first converted into grayscale before performing the feature extraction. The image feature is derived by concatenating the statistical estimator with the Gaussian, Laplace, and GGD assumptions over all SGF transformed sub-bands. In this experiment, Gaussian feature descriptor has a dimensionality of 96, in which the difference between two consecutive orientation angle is $\Delta\theta = 0.021\pi$. An orientation angle for all SGF basis filter lies between the range $[0, \pi]$. We employ K-Nearest Neighbor (KNN), Minimum Distance (MinDist), and Support Vector Machine (SVM) as the classifier to assign class label of testing image based on the Gaussian feature descriptor. Table 1 shows the vehicle verification performance of Gaussian, Laplace, and GGD feature descriptors for SGF-1 and SGF-2, respectively, over various vehicle poses and classifiers. As reported in these tables, the SVM classifier yields the best performance

over all proposed feature descriptors.

Table 1
Performance of the Proposed Method over Various Classifiers

Feature Descriptor	KNN-L1	KNN-L2	MinDis	SVM
$F_{\mu\sigma}$ SGF-1	99.86	97.76	93.78	**99.98**
$F_{\mu\lambda}$ SGF-1	99.85	99.85	93.39	**99.96**
$F_{\alpha\beta}$ SGF-1	97.9	98.04	82.4	**98.96**
$F_{\mu\sigma}$ SGF-2	99.85	99.88	92.6	**99.98**
$F_{\mu\lambda}$ SGF-2	99.86	99.81	92.41	**99.92**
$F_{\alpha\beta}$ SGF-2	98.25	98.08	82.63	**99.22**

B. Comparison with the former existing methods

In this subsection, the effectiveness of the proposed feature descriptor is compared with the other former existing methods. Herein, the SVM is utilized as the baseline classifier for comparison. The experiment was conducted with the 5-fold 50% holdout cross-validation as suggested by [4]. In this experiment, the feature dimensionality is set at 48 for Gaussian, Laplace, and GGD descriptors. This dimensionality is identical to that of the [4-5]. The orientation angles for the SGF basis function are set in between $[0, \pi]$. The difference between two consecutive orientation angles of the SGF basis filter is $\Delta\theta = 0.042\pi$. Table 2 clearly reveals that the proposed method consistently outperforms the conventional schemes. Thus, the proposed feature descriptors can be a very effective and potential candidate in the vehicle verification task.

Table 2
Performance Comparisons between the Proposed Method and Former Existing Schemes

Method	Far	Left	Middle Close	Right	Average
PCA [2]	91.56	93.32	96.22	91.04	93.04
Reduced HOG [3]	92.44	96.48	95.36	95.64	94.98
LG [4]	91.6	97.18	98	96.96	95.94
HOG [3]	98.14	98.32	99.18	97.44	98.27
Gamma [5]	99.75	99.4	99.65	97.65	99.11
$F_{\mu\sigma}$ SGF-1	99.95	99.95	100	100	**99.98**
$F_{\mu\lambda}$ SGF-1	99.95	100	99.95	99.95	99.96
$F_{\alpha\beta}$ SGF-1	99.4	99.6	98.4	98.45	98.96
$F_{\mu\sigma}$ SGF-2	100	99.95	99.95	100	**99.98**
$F_{\mu\lambda}$ SGF-2	99.85	99.9	99.95	100	99.92
$F_{\alpha\beta}$ SGF-2	99.15	99.3	98.7	99.75	99.22

Figure 4 shows some vehicle verification results using the proposed feature descriptor. As it can be seen, the proposed vehicle verification improves the detection result of the on-road vehicle objects. The vehicle verification is able to classify the correct vehicle and non-vehicle hypothesis which can further refine the vehicle detection result.

V. CONCLUSION

In this paper, a new method has been presented to construct the feature descriptor for the vehicle verification task. Specifically, an image feature descriptor is composed of the statistical parameters of the SGF filtered output under a heavy-tailed bell-shape distribution modeling. As documented in experimental results, the proposed feature descriptor is superior to the former methods in terms of the vehicle verification task.

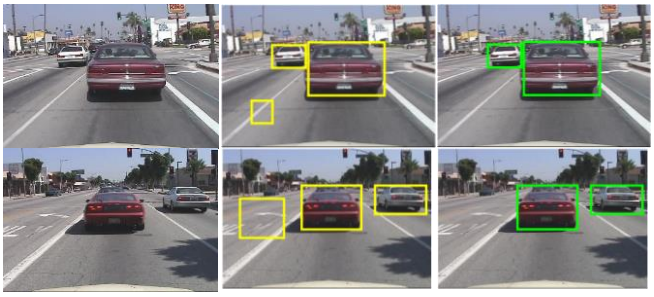

Figure 4: Examples of vehicle detection and verification result: (first column) input image, (second column) vehicle hypothesis generation, and (third column) vehicle hypothesis verification using $F_{\mu\sigma}$ SGF-2

ACKNOWLEDGMENT

This research is fully funded by Universitas Sebelas Maret (UNS), Surakarta, Indonesia under grant contract 1075/UN27.21/PP/2017 (MRG PKLP UNS - PNBP Saldo Awal Batch 2).

REFERENCES

[1] Z. Sun, G. Bebis, and R. Miller, "On-road vehicle detection: a review," *IEEE Trans. Pattern Anal. Mach. Intell.*, vol. 28, no. 5, pp. 694-711, May 2006.

[2] J. Zhou, D. Gao, and D. Zhang, "Moving vehicle detection for automatic traffic monitoring," *IEEE. Trans. Veh. Tech.*, vol. 56., no. 1, pp. 51-59, Jan. 2007.

[3] N. Dalal, and B. Triggs, "Histograms of oriented gradients for human detection," in *Proc. IEEE Comput. Soc. Conf. Comput. Vis. Pattern Recognit.*, vol. 1, pp. 886-893, 2005.

[4] J. Arrospide, and L. Salgado, "Log-Gabor filters for image-based vehicle verification," *IEEE. Trans. Image Process.*, vol. 22, no. 6, pp. 2286-2295, Jun. 2013.

[5] J.-M. Guo, H. Prasetyo, and K. Wong, "Vehicle verification using Gabor filter magnitude with Gamma Distribution Modeling," *IEEE Signal Process. Lett.*, vol. 21, no. 5, pp. 600-604, 2014.

[6] Z. Sun, R. Miller, G. Bebis, and D. Dimeo, "A real-time precrash vehicle detection system," in *Proc. 6thIEEE Workshop on Applications of Computer Vision*, pp. 171-176, 2002.

[7] Z. Sun, G. Bebis, and R. Miller, "On-road vehicle detection using evolutionary Gabor filter optimization," *IEEE Trans. Intell. Transp. Syst.*, vol. 6, no. 2, pp. 125-137, Jun. 2005.

[8] Z. Sun, G. Bebis, and R. Miller, "Monocular precrash vehicle detection: features and classifier," *IEEE. Trans. Image Process.*, vol. 15, no. 7, pp. 2019-2034, Jul. 2006.

[9] W. T. Freeman, and E. H. Adelson, "The design and use of steerable filters," *IEEE Trans. Pattern Anal. Mach. Intell.*, vol. 13, no. 9, pp. 891-906, Sep. 1991.

[10] W. Beil, "Steerable filters and invariance theory," *Pattern Recog. Lett.*, vol. 15., no. 5, pp. 453-460, May 1994.

[11] E. P. Simoncelli and H. Farid, "Steerable wedge filters for local orientation analysis," *IEEE Trans. Image Process.*, vol. 5, no. 9, pp. 1377–1382, Sep. 1996.

[12] GTI Vehicle Image Database, (2011), [Online] Available: http://www.gti.ssr.upm.es/data/